
PET Imaging Analysis with ^{64}Cu in Disulfiram Treatment for Aberrant Copper Biodistribution in Menkes Disease Mouse Model

Shiho Nomura¹, Satoshi Nozaki², Takashi Hamazaki¹, Taisuke Takeda¹, Eiichi Ninomiya¹, Satoshi Kudo¹, Emi Hayashinaka², Yasuhiro Wada², Tomoko Hiroki³, Chie Fujisawa³, Hiroko Kodama³, Haruo Shintaku¹, and Yasuyoshi Watanabe²

¹Department of Pediatrics, Graduate School of Medicine, Osaka City University, Osaka, Japan; ²RIKEN Center for Life Science Technologies, Kobe, Japan; and ³Department of Pediatrics, School of Medicine, Teikyo University, Tokyo, Japan

Menkes disease (MD), an X-linked recessive disorder of copper metabolism caused by mutations in the copper-transporting *ATP7A* gene, results in growth failure and severe neurodegeneration in early childhood. Subcutaneous copper-histidine injection is the standard treatment for MD, but it has limited clinical efficacy. Furthermore, long-term copper injection causes excess copper accumulation in the kidneys, resulting in renal dysfunction. To attempt to resolve this issue, we used PET imaging with ^{64}Cu to investigate the effects of disulfiram on copper biodistribution in living mice serving as an animal model for MD (MD model mice). **Methods:** Macular mice were used as MD model mice, and C3H/He mice were used as wild-type mice. Mice were pretreated with 2 types of chelators (disulfiram, a lipophilic chelator, and D-penicillamine, a hydrophilic chelator) 30 min before $^{64}\text{CuCl}_2$ injection. After $^{64}\text{CuCl}_2$ injection, emission scans covering the whole body were performed for 4 h. After the PET scans, the brain and kidneys were analyzed for radioactivity with γ counting and autoradiography. **Results:** After copper injection alone, marked accumulation of radioactivity (^{64}Cu) in the liver was demonstrated in wild-type mice, whereas in MD model mice, copper was preferentially accumulated in the kidneys (25.56 ± 3.01 percentage injected dose per gram [%ID/g]) and was detected to a lesser extent in the liver (13.83 ± 0.26 %ID/g) and brain (0.96 ± 0.08 %ID/g). Copper injection with disulfiram reduced excess copper accumulation in the kidneys (14.54 ± 2.68 %ID/g) and increased copper transport into the liver (29.42 ± 0.98 %ID/g) and brain (5.12 ± 0.95 %ID/g) of MD model mice. Copper injection with D-penicillamine enhanced urinary copper excretion and reduced copper accumulation in most organs in both mouse groups. Autoradiography demonstrated that disulfiram pretreatment induced copper transport into the brain parenchyma and reduced copper accumulation in the renal medulla. **Conclusion:** PET studies with ^{64}Cu revealed that disulfiram had significant effects on the copper biodistribution of MD. Disulfiram increased copper transport into the brain and reduced copper uptake in the kidneys of MD model mice. The application of ^{64}Cu PET for the treatment of MD and other copper-related disorders may be useful in clinical settings.

Key Words: Menkes disease; copper; PET; disulfiram; D-penicillamine

J Nucl Med 2014; 55:845–851

DOI: 10.2967/jnumed.113.131797

Menkes disease (MD) is an inherited X-linked disorder of copper metabolism caused by mutations in the *ATP7A* gene, which encodes a copper-transporting protein (1,2). *ATP7A* controls copper transport from the cytosol to the Golgi apparatus and copper excretion from cells (3). In patients with MD, dysfunctional *ATP7A* causes a failure of copper absorption from the intestine (4). Because macular mice possess a mutation in the mottled gene (*atp7a*) and have a clinical phenotype and biochemical abnormalities similar to those of MD patients, they can serve as an animal model for MD (i.e., MD model mice) (5–7). Systemic copper deficiency was demonstrated to cause dysfunction of copper-dependent enzymes and to result in multisystem disorders, such as severe neurodegeneration, connective tissue abnormalities, and kinky hair, in these mice (8,9).

To correct systemic copper deficiencies in MD, subcutaneous copper-histidine injection is the standard treatment (10–12), but its efficacy depends on the age-related maturation of the blood–brain barrier (BBB) or residual copper transport by a partially functional gene (12–14). When copper treatment is initiated in the neonatal period or early infancy, when the BBB is immature, the injected copper is delivered to the neurons and, thus, is an effective treatment for neurologic disorders (11,14). However, parenteral copper administration has limited clinical efficacy in MD patients more than 2 mo old because the injected copper is trapped in the maturing BBB (11).

Another important aspect of parenteral copper administration is that copper treatment is sometimes associated with excess copper accumulation in the kidneys, leading to renal dysfunction in patients and macular mice with MD (6,15). Previous reports demonstrated that copper administration lengthened the life-span of MD model mice but that copper accumulation to toxic levels in the kidneys led to severe renal damage (16,17). The mechanisms of copper-induced renal damage have not been fully elucidated; however, the oxidative potential of copper is considered to induce free-radical production and to result in cellular damage (18,19). To date, there have been no studies on the development of a treatment focusing on the prevention of copper accumulation in the kidneys.

Received Aug. 30, 2013; revision accepted Jan. 1, 2014.

For correspondence or reprints contact: Yasuyoshi Watanabe, RIKEN Center for Life Science Technologies, 6-7-3 Minatojima-minamimachi, Chuo-ku, Kobe, Hyogo 650-0047, Japan.

E-mail: yywata@riken.jp

Published online Mar. 13, 2014.

COPYRIGHT © 2014 by the Society of Nuclear Medicine and Molecular Imaging, Inc.

Several attempts have been made to develop novel methods to address insufficient copper transport into the brain in the presence of a maturing BBB. Kodama et al. (20) and Munakata et al. (21) demonstrated that the use of a combination of copper and disulfiram, a lipophilic chelator, improved copper deficiency in the brain of MD model mice (macular mice). Administered disulfiram is immediately converted into sodium diethyldithiocarbamate (DEDTC) by glutathione reductase, and the complex of copper and DEDTC can pass through the BBB (22–24). To advance these findings to clinical application, it is important to elucidate the time course of copper biodistribution with and without disulfiram. Therefore, an evaluation of disulfiram via pharmacology safety studies, such as absorption, distribution, metabolism, and excretion studies, must be performed in an animal model before clinical trials in humans. Traditionally, the evaluation of absorption, distribution, metabolism, and excretion in the development of pharmaceuticals has involved autoradiography of the whole body and the detection of radioactivity associated with dissected tissues by use of radioactive ^{125}I - or ^{111}In -labeled pharmaceuticals (25). However, recently developed molecular imaging technologies allow the visualization and quantitative measurement of biologic processes in living systems (26–28). Radioisotope-based molecular imaging techniques, such as PET, have been used for the non-invasive detection of pharmacodynamics in the gut and for the determination of functional changes in the nervous system (26,27).

In this study, we aimed to investigate the effects of 2 types of copper chelators (disulfiram, a lipophilic chelator, and D-penicillamine, a hy-

drophilic chelator) on copper biodistribution after copper injection in MD model mice by PET imaging with ^{64}Cu .

MATERIALS AND METHODS

Animals and Disulfiram and D-Penicillamine Pretreatments

This study was performed in accordance with international standards for animal welfare and institutional guidelines and was approved by the animal care and use committees of Osaka City University, Osaka, Japan, and RIKEN Center for Life Science Technologies, Kobe, Japan. We used 4- to 7-wk-old C3H/He mice (body weight, 16–24 g) purchased from Japan SLC as wild-type mice and 4- to 8-wk-old macular mice (7–22 g) bred at Teikyo University as MD model mice (5–7).

Mice were anesthetized with a mixture of 1.5% isoflurane (Abbott), nitrous oxide (0.5 L/min), and 100% oxygen (1.5 L/min). In mice pretreated with disulfiram (100 mg/kg; Wako Pure Chemicals), disulfiram diluted with sesame oil was injected intraperitoneally. In mice pretreated with D-penicillamine (100 mg/kg; Wako Pure Chemicals), D-penicillamine diluted with saline was injected subcutaneously.

$^{64}\text{CuCl}_2$ PET

$^{64}\text{CuCl}_2$ was produced from the cyclotron at the RIKEN Center for Life Science Technologies. At 30 min after disulfiram or D-penicillamine pretreatment, $^{64}\text{CuCl}_2$ corresponding to an activity of 30 MBq was administered via the tail vein. Mice were imaged in the prone position in a small-animal PET scanner (microPET Focus220; Siemens Medical Solutions Inc.). Continuous PET scanning was performed for 4 h immediately after $^{64}\text{CuCl}_2$ injection. PET data were acquired in the list mode and reconstructed by use of a filtered backprojection algorithm with a ramp filter cutoff at the Nyquist frequency, attenuation correction, and no scatter correction. The PET image data were displayed and analyzed with IDL VM 6.3 (Exelis Inc.) and ASIPro VM (Siemens Medical Solutions Inc.) software. Regions of interest were drawn manually on PET images, and the percentage injected dose per gram of tissue (%ID/g) was calculated with the software. Three mice were scanned for each experimental group, and data from these mice were subjected to statistical analysis.

Regions of interest were drawn manually on PET images, and the percentage injected dose per gram of tissue (%ID/g) was calculated with the software. Three mice were scanned for each experimental group, and data from these mice were subjected to statistical analysis.

γ Counting and Ex Vivo Autoradiography

^{64}Cu accumulation was evaluated by γ counting at 4 h after $^{64}\text{CuCl}_2$ injection as described previously (29). Each sample was counted in a 1470 WIZARD automatic γ counter (Wallac). Tissues were weighed, and the amount of radioactivity was calculated as the %ID/g. Six wild-type mice and 4 MD model mice were included in each experimental group, and data from these mice were subjected to statistical analysis.

For the quantification of emission data, ex vivo brain and renal autoradiography was performed as described previously (26). Brain tissue was sliced into coronal sections and kidney tissue was sliced into sagittal sections (1 mm thick) with a brain matrix (RBM-2000C; ASI instruments Inc.). Brain and kidney slices were placed on an imaging plate (BAS-SR2040; Fuji Photo Film) for 15 and 5 min, respectively. Exposed imaging plates

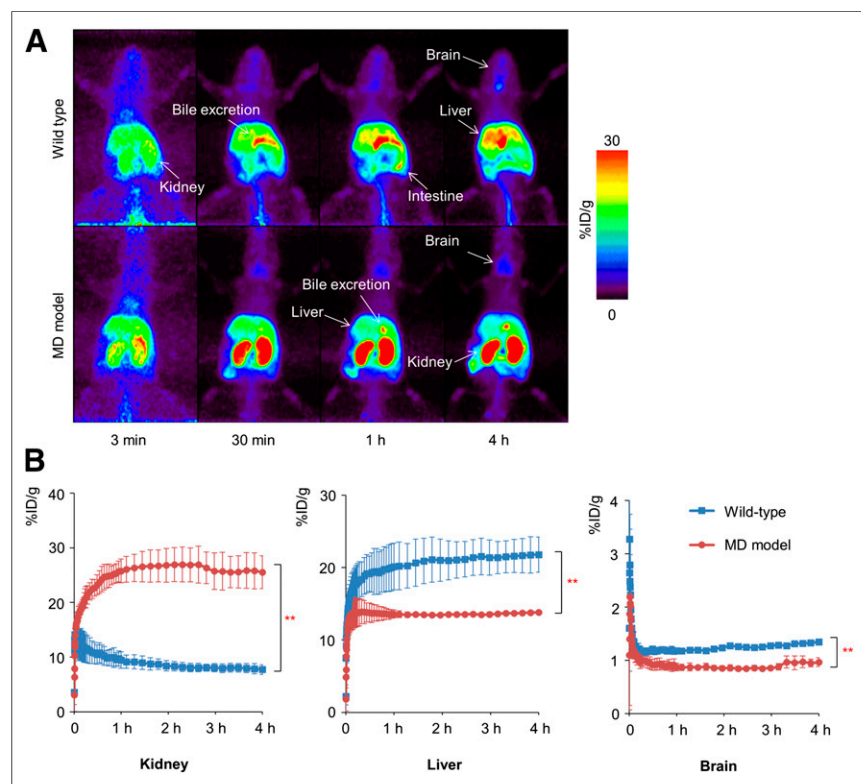


FIGURE 1. PET image analysis after $^{64}\text{CuCl}_2$ injection in wild-type and MD model mice. (A) Coronal section of whole-body PET image 4 h after $^{64}\text{CuCl}_2$ injection in MD model mice. (B) Time-activity curve for kidneys, liver, and brain 4 h after $^{64}\text{CuCl}_2$ injection. MD model mice showed higher level of copper accumulation in kidneys and lower levels of copper accumulation in liver and brain than wild-type mice. $**P < 0.01$.

were scanned with an imaging analyzer (FLA-7000; Fuji). Reproducibility was confirmed in 3 independent experiments.

Statistical Analyses

All data are presented as mean \pm SD. Statistical analyses were performed with commercially available software (JMP version 9; SAS Institute). Statistical analyses of PET data with time-activity curves were performed with repeated-measures ANOVA. Statistical analyses of γ -counting data were performed with the Wilcoxon test.

RESULTS

Copper Accumulation without Chelator in Wild-Type and MD Model Mice

In wild-type mice, copper uptake in the kidneys was confirmed soon after copper injection, reached a maximum level, and gradually decreased (7.74 ± 0.90 %ID/g at 4 h). Copper excretion into bile could be seen, and we detected copper uptake in the intestine. The marked copper uptake in the liver continued to increase during PET imaging (21.80 ± 2.42 %ID/g at 4 h). In the brain, copper uptake was low but increased gradually during PET imaging (1.34 ± 0.03 %ID/g at 4 h) (Fig. 1).

In MD model mice, copper uptake in the kidneys was markedly elevated (25.56 ± 3.01 %ID/g at 4 h) and was 4-fold higher than that in wild-type mice ($P < 0.01$). Copper excretion into bile was evident, and copper uptake in the liver was maintained at a plateau (13.83 ± 0.26 %ID/g at 4 h). Copper uptake in the brain was lower (0.96 ± 0.08 %ID/g at 4 h) than that in the kidneys and liver and was significantly lower than that in wild-type mice ($P < 0.01$) (Fig. 1).

The γ -counting data supported the PET scan data showing that copper uptake in the kidneys of MD model mice was significantly higher than that in wild-type mice (14.47 ± 3.39 %ID/g in wild-type mice and 84.38 ± 12.39 %ID/g in MD model mice; $n = 4-6$; $P < 0.05$). On the other hand, copper uptake in the liver of MD model mice was significantly lower than that in wild-type mice (38.80 ± 3.46 %ID/g in wild-type mice and 22.27 ± 1.93 %ID/g in MD model mice; $n = 4-6$; $P < 0.05$). Copper uptake in the

brain in both wild-type and MD model mice was low, with no significant differences (Table 1).

These data confirmed that systemic copper injection without chelator resulted in marked copper accumulation in the kidneys of MD model mice. The uptake of injected copper in the liver and brain of MD model mice was lower than that in wild-type mice.

Effects of Disulfiram or D-Penicillamine Pretreatment in Wild-Type Mice

There were no significant differences in copper uptake in the kidneys of mice pretreated with disulfiram and mice not pretreated with the chelator. In the liver, disulfiram pretreatment increased copper uptake (28.82 ± 7.62 %ID/g at 4 h). In the brain, copper uptake was gradually elevated during PET imaging (5.32 ± 0.03 %ID/g at 4 h), and there were significant differences between mice receiving and mice not receiving disulfiram pretreatment ($P < 0.01$) (Fig. 2). On the other hand, D-penicillamine pretreatment significantly reduced copper uptake in the kidneys compared with that in mice not pretreated with the chelator ($P < 0.01$). Copper uptake in the liver and brain at 4 h was markedly lower in mice pretreated with D-penicillamine (6.80 ± 1.22 %ID/g in the liver and 0.40 ± 0.08 %ID/g in the brain) than in those not pretreated with the chelator ($P < 0.01$) (Figs. 2A and 2C).

The γ -counting data confirmed that disulfiram pretreatment increased copper accumulation in the brain, heart, liver, spleen, muscle, and blood and decreased it in the stomach, intestine, and kidneys of wild-type mice. D-Penicillamine enhanced urinary copper excretion and decreased copper accumulation in all organs investigated (Table 1).

These data confirmed that disulfiram increased copper accumulation in the brain and liver but did not alter copper accumulation in the kidneys of wild-type mice. D-Penicillamine strongly enhanced urinary copper excretion in wild-type mice.

Effects of Disulfiram or D-Penicillamine Pretreatment in MD Model Mice

Copper accumulation in the kidneys of MD model mice at 4 h was significantly lower in mice pretreated with disulfiram or

TABLE 1
 γ -counting Data for Each Organ 4 Hours After $^{64}\text{CuCl}_2$ Injection

Organ	Mean \pm SD %ID/g for:					
	Wild-type mice			MD model mice		
	No chelator ($n = 6$)	Disulfiram ($n = 6$)	D-Penicillamine ($n = 6$)	No chelator ($n = 4$)	Disulfiram ($n = 4$)	D-Penicillamine ($n = 4$)
Brain	1.00 \pm 0.17	7.89 \pm 1.08*	0.34 \pm 0.05*	1.21 \pm 0.19	4.73 \pm 2.74*	0.44 \pm 0.16*
Heart	6.87 \pm 1.50	12.99 \pm 6.06*	2.06 \pm 0.28*	2.17 \pm 0.18†	10.36 \pm 5.19‡	2.09 \pm 1.48
Lungs	19.39 \pm 5.02	16.36 \pm 2.15	5.28 \pm 2.25*	8.86 \pm 1.35†	11.62 \pm 4.77	2.38 \pm 0.55‡
Liver	38.80 \pm 3.46	61.61 \pm 13.51‡	14.04 \pm 2.96*	22.27 \pm 1.93†	31.11 \pm 15.06	16.04 \pm 2.96‡
Pancreas	6.28 \pm 1.42	8.75 \pm 3.00	2.73 \pm 0.66*	2.33 \pm 1.15†	5.14 \pm 2.83	1.56 \pm 0.81
Spleen	5.28 \pm 1.13	8.91 \pm 2.40*	1.62 \pm 0.56*	4.03 \pm 0.17	5.66 \pm 2.37	2.65 \pm 1.15
Stomach	30.01 \pm 12.81	6.45 \pm 1.33*	11.89 \pm 1.89*	29.61 \pm 6.63	5.91 \pm 3.58*	9.25 \pm 2.82*
Intestine	18.02 \pm 3.45	6.17 \pm 1.29*	6.83 \pm 1.15*	21.89 \pm 2.12	4.67 \pm 1.72‡	8.71 \pm 2.93‡
Kidneys	14.47 \pm 3.39	15.31 \pm 2.34	9.76 \pm 1.32‡	84.38 \pm 12.39†	22.46 \pm 9.64‡	45.46 \pm 17.54
Muscle	0.81 \pm 0.24	2.18 \pm 1.03*	0.47 \pm 0.35	0.59 \pm 0.05	1.34 \pm 0.98	0.33 \pm 0.29
Blood	3.01 \pm 0.74	6.04 \pm 1.02*	1.15 \pm 0.40*	1.64 \pm 0.27†	1.50 \pm 0.17	1.11 \pm 0.10‡
Urine	5.04 \pm 3.05	0.34 \pm 0.12*	199.24 \pm 123.42*	4.75 \pm 0.96	0.40 \pm 0.44‡	384.62 \pm 380.52‡

* $P < 0.01$ for no chelator vs. disulfiram or D-penicillamine in wild-type or MD model mice.

† $P < 0.05$ for no chelator in wild-type mice vs. no chelator in MD model mice.

‡ $P < 0.05$ for no chelator vs. disulfiram or D-penicillamine in wild-type or MD model mice.

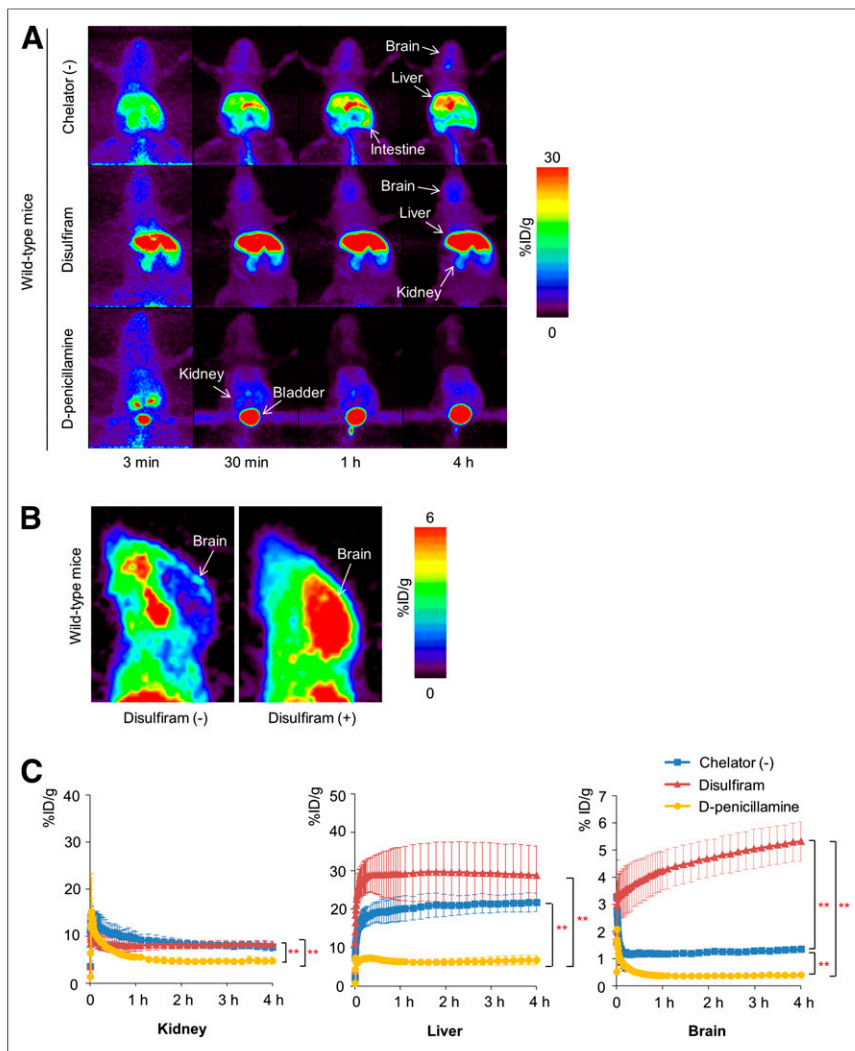


FIGURE 2. PET image analysis after $^{64}\text{CuCl}_2$ injection and disulfiram or D-penicillamine pretreatment in wild-type mice. (A) Coronal section of whole-body PET image 4 h after $^{64}\text{CuCl}_2$ injection in wild-type mice. Chelator (-) = no chelator. (B) Sagittal section of brain PET image 4 h after $^{64}\text{CuCl}_2$ injection. (C) Time-activity curve for kidneys, liver, and brain 4 h after $^{64}\text{CuCl}_2$ injection. In wild-type mice, disulfiram increased copper accumulation in liver and brain, and D-penicillamine enhanced urinary copper excretion and decreased copper accumulation in all organs. Data are mean \pm SD. $**P < 0.01$.

D-penicillamine than in mice not pretreated with a chelator (14.54 ± 2.68 %ID/g in mice pretreated with disulfiram and 16.71 ± 2.89 %ID/g in mice pretreated with D-penicillamine) ($P < 0.05$). On the other hand, disulfiram pretreatment significantly increased copper accumulation in the liver (29.42 ± 0.98 %ID/g) and brain (5.12 ± 0.95 %ID/g) at 4 h compared with that in mice not pretreated with the chelator ($P < 0.01$). D-Penicillamine pretreatment decreased copper accumulation in the brain and liver ($P < 0.01$) (Fig. 3).

The γ -counting data confirmed that disulfiram pretreatment increased copper accumulation in the brain and heart and decreased it in the stomach, intestine, and kidneys of MD model mice. D-Penicillamine enhanced urinary copper excretion and decreased copper accumulation in most organs investigated (Table 1).

These data confirmed that disulfiram increased copper accumulation in the brain and liver and decreased copper accumulation in the kidneys of MD model mice. D-Penicillamine strongly enhanced

urinary copper excretion and decreased copper accumulation in the kidneys, brain, and liver of MD model mice.

Brain Autoradiography

At 4 h after copper administration without a chelator, high levels of copper accumulation were observed in the lateral ventricle and the third ventricle in wild-type mice. MD model mice showed a similar pattern of copper accumulation, but the overall level of copper accumulation was lower than that in wild-type mice. Disulfiram pretreatment markedly increased copper uptake in the brain parenchyma in both wild-type and MD model mice. High levels of copper uptake were observed in the cerebral cortex and thalamus, whereas copper uptake in the ventricles was not prominent (Fig. 4A).

Renal Autoradiography

Compared with wild-type mice, MD model mice showed marked accumulation of injected copper in the renal tissue and notable accumulation in both the cortex and the medulla. Both chelators (disulfiram and D-penicillamine) decreased copper uptake in the renal tissue of MD model mice, but the copper distribution patterns in the disulfiram and D-penicillamine pretreatment groups were different. Disulfiram decreased copper uptake in the medulla, whereas D-penicillamine decreased it in the cortex (Fig. 4B).

DISCUSSION

PET is a functional imaging technique with high sensitivity. With the development of dedicated small-animal PET scanners, it is possible to perform functional imaging in small animals at high spatial resolutions (26–28). Using a small-animal PET imaging system, we obtained the first evidence—to our knowledge—that disulfiram pretreatment efficiently corrects inappropriate copper biodistribution in living MD model mice. The dynamics of administered copper and the time course of the effects of disulfiram in living animals strengthen the results of previous studies demonstrating the effects of disulfiram with conventional methods, such as histochemistry in postmortem animals (20,23). These data accelerate our goal—the clinical application of disulfiram treatment in MD patients.

For macular mice, well-established as an MD model, the present study confirmed that copper accumulation after systemic copper injection without a chelator shifted to the kidneys rather than the liver and brain, as in wild-type mice; these findings are consistent with previous findings for MD patients and MD model mice (2,12). Copper deficiency in the brain due to copper transport dysfunction at the BBB causes severe neurodegeneration in MD (8); therefore, it is important to develop an effective strategy for improving copper transport into the brain on the basis of copper

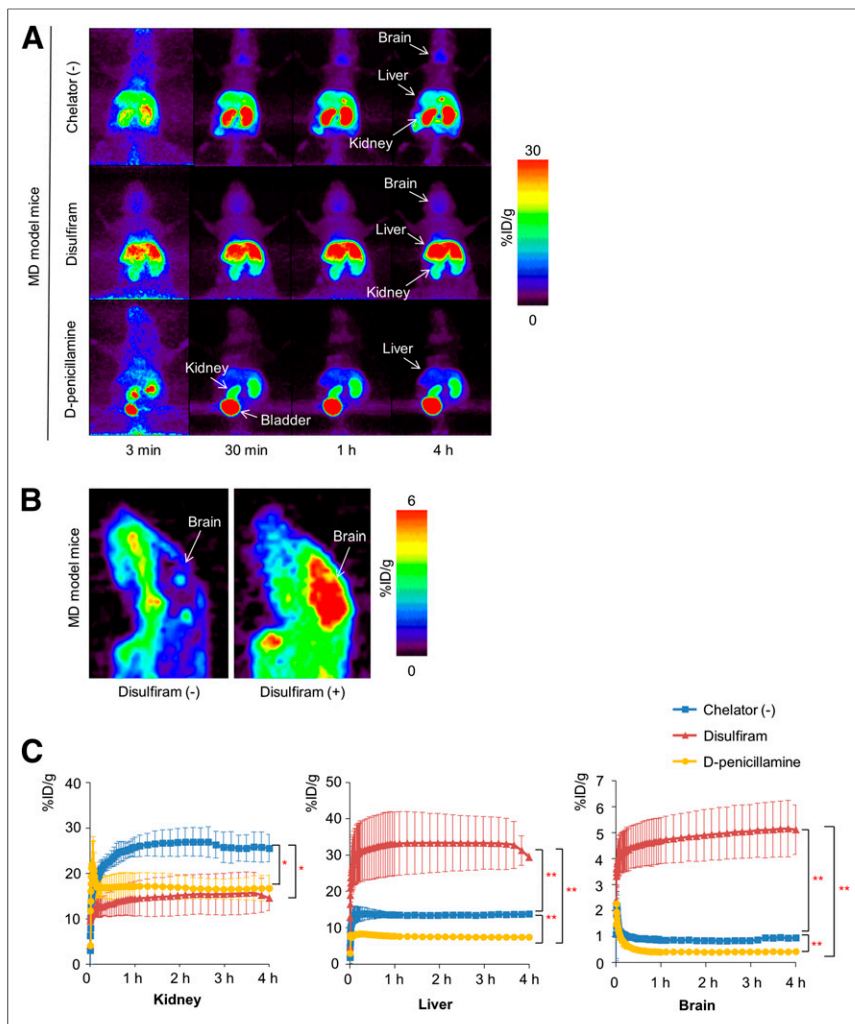


FIGURE 3. PET image analysis after $^{64}\text{CuCl}_2$ injection and disulfiram or D-penicillamine pretreatment in MD model mice. (A) Coronal section of whole-body PET image 4 h after $^{64}\text{CuCl}_2$ injection. Chelator (-) = no chelator. (B) Sagittal section of brain PET image 4 h after $^{64}\text{CuCl}_2$ injection. (C) Time-activity curve for kidneys, liver, and brain 4 h after $^{64}\text{CuCl}_2$ injection. In MD model mice, disulfiram decreased copper accumulation in kidneys and increased copper accumulation in liver and brain, and D-penicillamine enhanced urinary copper excretion and decreased copper accumulation in all organs. Data are mean \pm SD. * $P < 0.05$. ** $P < 0.01$.

dynamics in living systems. PET imaging provided direct visual evidence that disulfiram rapidly increased copper uptake in the brain of MD model mice on the basis of copper dynamics, including the detailed time course of copper transport in the whole body of a living mouse. Our quantitative time-activity curve analysis was sensitive enough to detect defective copper uptake in the brain parenchyma of MD model mice, which could not be evaluated by conventional γ counting because of high background activity from the periventricular vasculature (Figs. 1B and 4A; Table 1). The effectiveness of disulfiram pretreatment and details about copper dynamics would contribute to accelerating human clinical trials of disulfiram therapy for MD patients. On the other hand, excess copper transport may pose a risk for free-radical production, resulting in cellular damage (18). Further study is needed to determine how to modulate copper transport to the brain to normalize neurologic function in MD patients with various background factors, such as age and gene mutation type. PET imaging is effective for evaluating safe doses of copper or disulfiram for the

maintenance of appropriate copper accumulation in the brain in living MD mice and humans.

With regard to the mechanisms responsible for the effects of disulfiram on copper transport into the brain, the hydrophobicity of DEDTC—an active and converted form of disulfiram—is known to allow the complex of DEDTC and copper to permeate cellular membranes, including the Golgi apparatus (20,23,30). However, the formation of the complex was not demonstrated *in vivo* in those studies. An alternative mechanism of copper transport (e.g., Ctr1) could not be ruled out as an explanation for the effects of disulfiram on copper transport. Our *ex vivo* brain autoradiography findings clearly demonstrated that the copper injected with disulfiram passed through the BBB and was taken up into the brain parenchyma. Interestingly, we found that copper uptake was most prominent in the thalamus and then in the cerebellar cortex. As for the regional differences in copper biodistribution, Szerdahelyi and Kása (22) demonstrated that the effects of a lipophilic chelator depended on the brain region, with the highest increase being observed in the hippocampus. Their histochemistry study also revealed increased accumulation of copper in the glia and neurons. The bioavailability of chelator-bound copper is crucial for clinical application. A recent study demonstrated that disulfiram treatment increased cuproenzyme (cytochrome *c* oxidase) activity in the brain, and the authors suggested that the transported copper was indeed bioavailable after disulfiram treatment (30). On the basis of the findings of present and previous studies, detailed data for copper biodistribution in the brain remain controversial; therefore, further evidence of copper biodistribution

in the brain should be gathered with PET imaging and other basic technologies.

Another important aspect of the present study was the significant disulfiram-mediated reduction of copper accumulation in the kidneys of MD model mice. Long-term copper injection has a risk of causing copper accumulation to toxic levels in the kidneys, leading to severe renal damage (15–17). The present study confirmed that, without disulfiram pretreatment, systemically administered copper was preferentially taken up by the kidneys of living MD model mice. PET imaging analysis confirmed that disulfiram pretreatment markedly improved aberrant copper accumulation in the kidneys, thus reducing the risk of renal complications associated with long-term copper treatment. A previous study demonstrated the efficacy of disulfiram treatment in mice but revealed excess copper accumulation in the kidneys (30). Differences in the dose and route of administration of copper and disulfiram, the timing of disulfiram administration, and the age of the animals tested may be responsible for the inconsistent

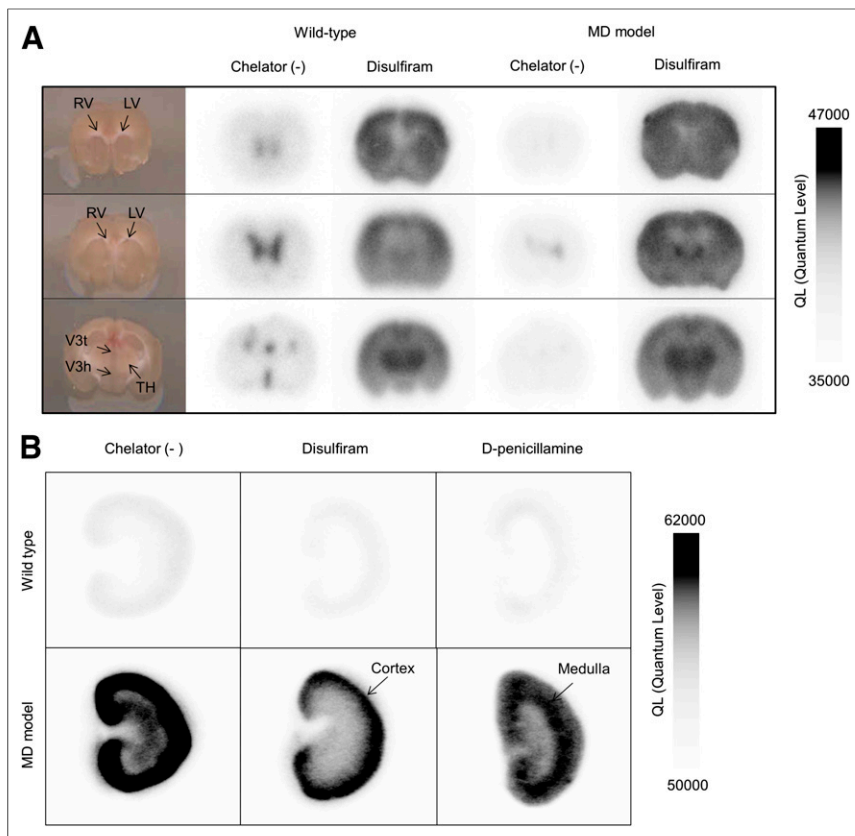


FIGURE 4. Autoradiography results. (A) Brain autoradiography after $^{64}\text{CuCl}_2$ injection. Disulfiram pretreatment increased uptake of $^{64}\text{CuCl}_2$ in cortex and thalamus. Chelator (-) = no chelator; LV = left ventricle; RV = right ventricle; TH = thalamus; V3t = thalamic part of third ventricle; V3h = hypothalamic part of third ventricle. (B) Renal autoradiography 4 h after $^{64}\text{CuCl}_2$ injection (sagittal sections). Disulfiram decreased copper accumulation in medulla, and D-penicillamine decreased copper accumulation in cortex.

results of the present study and previous studies. Because copper is usually administered subcutaneously in clinical settings, it is important to compare biodistributions achieved with various routes of administration (31). Further study is needed to establish effective and safe treatment with disulfiram and the PET imaging system in living animals.

In MD patients, primary renal dysfunction is caused by copper accumulation mainly in the medulla (renal tubule) (15); therefore, the finding that disulfiram was able to reduce copper uptake in the medulla was significant. Our ex vivo autoradiography analysis of the kidneys with 2 types of chelators revealed different copper distribution patterns in renal tissue: disulfiram-mediated reduction of copper uptake in the medulla and D-penicillamine-mediated reduction of copper uptake in the cortex. These observations further suggest the efficacy of the use of the combination of copper and disulfiram in MD patients.

CONCLUSION

The present PET imaging study clarified that disulfiram pretreatment provided 2 favorable outcomes for copper replacement therapy in MD model mice: increased copper uptake in the brain and reduced copper uptake in the kidneys. Our findings strongly suggest that copper-chelating agents can act as nonenzymatic transporters of copper to correct the biodistribution of copper in

MD patients. Noninvasive PET imaging is useful for visualizing and quantifying copper dynamics, accelerating the clinical application of copper chelators for MD.

DISCLOSURE

The costs of publication of this article were defrayed in part by the payment of page charges. Therefore, and solely to indicate this fact, this article is hereby marked "advertisement" in accordance with 18 USC section 1734. This study was supported by a grant for research on intractable diseases from MHLW of Japan (H23-nannchi-ippann-091) and JSPS KAKENHI grant 24591523. No other potential conflict of interest relevant to this article was reported.

ACKNOWLEDGMENTS

We thank Daisuke Tokuhara, MD, PhD, and Hiroki Fujioka, MD, PhD, for their efforts.

REFERENCES

1. Vulpe C, Levinson B, Whitney S, Packman S, Gitschier J. Isolation of a candidate gene for Menkes disease and evidence that it encodes a copper-transporting ATPase. *Nat Genet.* 1993;3:7-13.
2. Kodama H, Murata Y. Molecular genetics and pathophysiology of Menkes disease. *Pediatr Int.* 1999;41:430-435.
3. Lutsenko S, Barnes NL, Bartee MY, Dmitriev OY. Function and regulation of human copper-transporting ATPases. *Physiol Rev.* 2007;87:1011-1046.
4. Kodama H, Abe T, Takama M, Takahashi I, Kodama M, Nishimura M. Histochemical localization of copper in the intestine and kidney of macular mice: light and electron microscopic study. *J Histochem Cytochem.* 1993;41:1529-1535.
5. Kodama H, Meguro Y, Abe T, et al. Genetic expression of Menkes disease in cultured astrocytes of the macular mouse. *J Inherit Metab Dis.* 1991;14:896-901.
6. Shiraishi N, Aono K, Taguchi T. Copper metabolism in the macular mutant mouse: an animal model of Menkes's kinky-hair disease. *Biol Neonate.* 1988;54:173-180.
7. Murata Y, Kodama H, Abe T, et al. Mutation analysis and expression of the mottled gene in the macular mouse model of Menkes disease. *Pediatr Res.* 1997;42:436-442.
8. Kodama H, Murata Y, Kobayashi M. Clinical manifestations and treatment of Menkes disease and its variants. *Pediatr Int.* 1999;41:423-429.
9. Meguro Y, Kodama H, Abe T, Kobayashi S, Kodama Y, Nishimura M. Changes of copper level and cytochrome c oxidase activity in the macular mouse with age. *Brain Dev.* 1991;13:184-186.
10. Kreuder J, Otten A, Fuder H, et al. Clinical and biochemical consequences of copper-histidine therapy in Menkes disease. *Eur J Pediatr.* 1993;152:828-832.
11. Sarkar B, Lingertat-Walsh K, Clarke JT. Copper-histidine therapy for Menkes disease. *J Pediatr.* 1993;123:828-830.
12. Wenk G, Suzuki K. The effect of copper supplementation on the concentration of copper in the brain of the brindled mouse. *Biochem J.* 1982;205:485-487.
13. Kaler SG, Das S, Levinson B, et al. Successful early copper therapy in Menkes disease associated with a mutant transcript containing a small in-frame deletion. *Biochem Mol Med.* 1996;57:37-46.
14. Christodoulou J, Danks DM, Sarkar B, et al. Early treatment of Menkes disease with parenteral copper-histidine: long-term follow-up of four treated patients. *Am J Med Genet.* 1998;76:154-164.
15. Kodama H, Okabe I, Kihara A, Mori Y, Okaniwa M. Renal tubular function of patients with classical Menkes disease. *J Inherit Metab Dis.* 1992;15:157-158.

16. Lenartowicz M, Kowal M, Buda-Lewandowska D, Styrna J. Pathological structure of the kidney from adult mice with mosaic mutation. *J Inherit Metab Dis*. 2002;25:647–659.
17. Lenartowicz M, Windak R, Tylko G, Kowal M, Styrna J. Effects of copper supplementation on the structure and content of elements in kidneys of mosaic mutant mice. *Biol Trace Elem Res*. 2010;136:204–220.
18. Cai L, Li XK, Song Y, Cherian MG. Essentiality, toxicology and chelation therapy of zinc and copper. *Curr Med Chem*. 2005;12:2753–2763.
19. Lutsenko S, Petris MJ. Function and regulation of the mammalian copper-transporting ATPases: insights from biochemical and cell biological approaches. *J Membr Biol*. 2003;191:1–12.
20. Kodama H, Sato E, Gu YH, Shiga K, Fujisawa C, Kozuma T. Effect of copper and diethylthiocarbamate combination therapy on the macular mouse, an animal model of Menkes disease. *J Inherit Metab Dis*. 2005;28:971–978.
21. Munakata M, Kodama H, Fujisawa C, et al. Copper-trafficking efficacy of copper-pyruvaldehyde bis(*N*₄-methylthiosemicarbazone) on the macular mouse, an animal model of Menkes disease. *Pediatr Res*. 2012;72:270–276.
22. Szerdahelyi P, Kása P. Regional differences in the uptake of exogenous copper into rat brain after acute treatment with sodium diethylthiocarbamate: a histochemical and atomic absorption spectrophotometric study. *Histochemistry*. 1987;86:627–632.
23. Aaseth J, Sjøli NE, Førre O. Increased brain uptake of copper and zinc in mice caused by diethylthiocarbamate. *Acta Pharmacol Toxicol (Copenh)*. 1979;45:41–44.
24. Johansson B, Stankiewicz Z. Bis-(diethylthiocarbamate) copper complex: a new metabolite of disulfiram? *Biochem Pharmacol*. 1985;34:2989–2991.
25. Staud F, Nishikawa M, Morimoto K, Takakura Y, Hashida M. Disposition of radioactivity after injection of liver-targeted proteins labeled with ¹¹¹In or ¹²⁵I: effect of labeling on distribution and excretion of radioactivity in rats. *J Pharm Sci*. 1999;88:577–585.
26. Mizuma H, Shukuri M, Hayashi T, Watanabe Y, Onoe H. Establishment of in vivo brain imaging method in conscious mice. *J Nucl Med*. 2010;51:1068–1075.
27. Yamashita S, Takashima T, Kataoka M, et al. PET imaging of the gastrointestinal absorption of orally administered drugs in conscious and anesthetized rats. *J Nucl Med*. 2011;52:249–256.
28. Takashima T, Wu C, Takashima-Hirano M, et al. Evaluation of breast cancer resistance protein function in hepatobiliary and renal excretion using PET with ¹¹C-SC-62807. *J Nucl Med*. 2013;54:267–276.
29. Yamato M, Kataoka Y, Mizuma H, Wada Y, Watanabe Y. PET and macro- and microautoradiographic studies combined with immunohistochemistry for monitoring rat intestinal ulceration and healing processes. *J Nucl Med*. 2009;50:266–273.
30. Bhadhprasit W, Kodama H, Fujisawa C, Hiroki T, Ogawa E. Effect of copper and disulfiram combination therapy on the macular mouse, a model of Menkes disease. *J Trace Elem Med Biol*. 2012;26:105–108.
31. Martin SM, O'Donnell RT, Kukis DL, et al. Imaging and pharmacokinetics of ⁶⁴Cu-DOTA-HB22.7 administered by intravenous, intraperitoneal, or subcutaneous injection to mice bearing non-Hodgkin's lymphoma xenografts. *Mol Imaging Biol*. 2009;11:79–87.